Available online at www.sciencedirect.com
SCIENCE DIRECT®
ELSEVIER
Journal of Molecular Catalysis B: Enzymatic 24–25 (2003) 99–109
JOURNAL OF MOLECULAR CATALYSIS B: ENZYMATIC
www.elsevier.com/locate/molcatb

Key residue responsible for catalytic activities in the antibodies elicited against *N*-methyl mesoporphyrin

Yasuko Kawamura-Konishi [a,*], Rumie Sasaki [a], Masami Sugiyama [a], Hiroshi Hashimoto [a], Takako Kamo [a], Naoki Hosomi [a], Masaaki Yamazaki [b], Hiroyuki Tashiro [b], Haruo Suzuki [a]

[a] *Department of Biosciences, School of Science, Kitasato University, 1-15-1 Kitasato, Sagamihara, Kanagawa 228-8555, Japan*
[b] *Bioscience Research Laboratory, Fujiya Co. Ltd, 228 Soya, Hadano, Kanagawa 257-0031, Japan*

Received 8 May 2003; received in revised form 8 May 2003; accepted 7 June 2003

Abstract

Five catalytic and nine non-catalytic antibodies for insertion of a metal ion into porphyrin were generated by immunization with *N*-methyl mesoporphyrin (*N*-MMP) as hapten, which was designed to mimic the distortion of porphyrin toward a transition-state geometry in the reaction. In order to determine the features responsible for the catalytic activity, we characterized the properties of the catalytic and non-catalytic antibodies. The catalytic antibodies did not have higher affinity to *N*-MMP than the non-catalytic ones. All the antibodies, except one non-catalytic antibody, combined with ferric *N*-methyl mesoporphyrin (*N*-MMP-Fe) to form the respective antibody·*N*-MMP-Fe complex. The binding affinity of cyanide to ferric iron in the complexes agreed with that of free *N*-MMP-Fe, indicating that the protruding side of *N*-MMP-Fe in the complexes is exposed to solvents. All the complexes of the catalytic antibodies had a peroxidase-like activity, whereas those of the non-catalytic ones did not. This suggests that the metalation activity associates with the peroxidase-like one, so that there is a common residue acting as catalyst for both reactions. The amino acid sequence alignment shows that the catalytic antibodies contain a homologous heavy chain sequence in the third complementarity-determining region. Based on the results, the possibility that Asp(H96) in the region is the key residue responsible for the metalation and peroxidase-like activities is discussed.

Keywords: Catalytic antibody; Metalation; Peroxidase; Porphyrin

1. Introduction

Since the first catalytic antibodies were generated in 1986 [1,2], transition-state stabilization has been the most important and successful guiding principle for generating catalytic antibodies [3,4]. When mice are immunized with a transition-state analogue (TSA) for a reaction, a huge repertoire of antibodies is induced against the TSA. According to the conventional screening method, all the anti-TSA antibodies are purified from hybridoma cell culture or ascites fluid and then examined in catalytic activity. In many cases, a few of the antibodies accelerate the reaction, while most of them do not [3–6]. These facts have raised a question: what factor is responsible for the catalytic

* Corresponding author. Tel.: +81-42-7789410; fax: +81-42-7789942.
E-mail address: konisi@jet.sci.kitasato-u.ac.jp (Y. Kawamura-Konishi).

1381-1177/$ – see front matter © 2003 Elsevier B.V. All rights reserved.
doi:10.1016/S1381-1177(03)00134-6

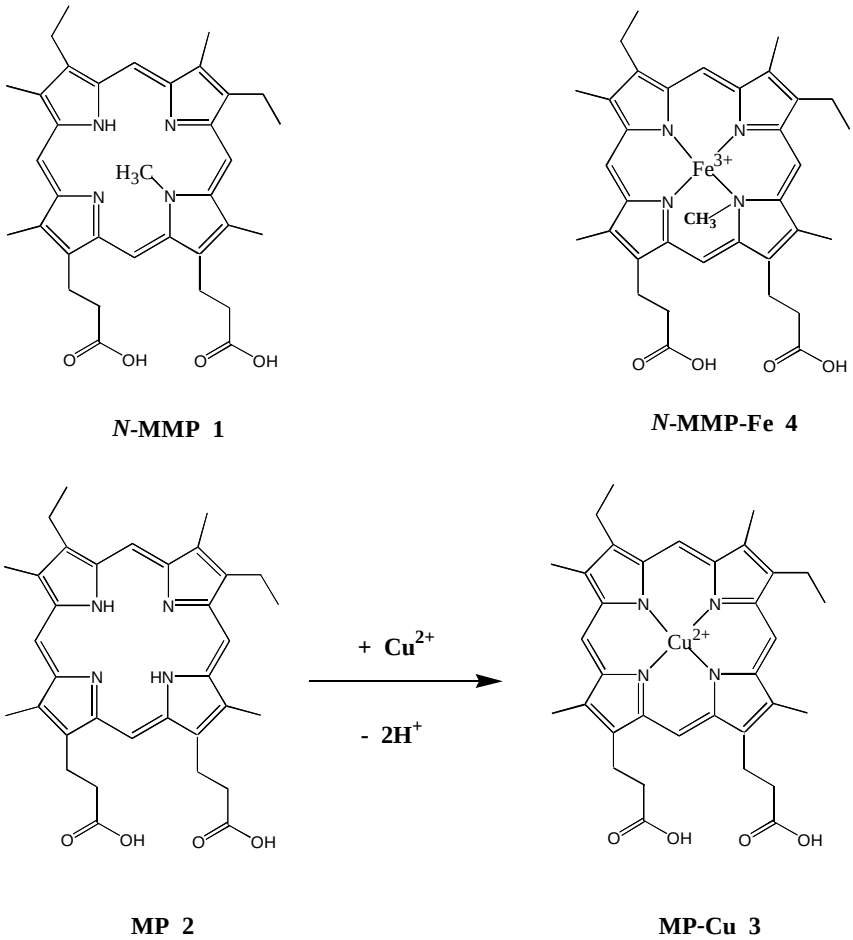

Fig. 1. Structures of hapten (*N*-methyl mesoporphyrin **1**), substrate (mesoporphyrin **2**), product (cupric-mesoporphyrin **3**), and ferric-*N*-methyl mesoporphyrin **4**.

activity besides the transition-state stabilization? The answer to this will help to understand the catalytic mechanism of the antibody and to produce an antibody with an enhanced catalytic activity.

Previously, we studied the immunization schedule for generation of polyclonal catalytic antibodies, and suggested that prolonged immunization by TSA, even after the TSA-binding activity reached a plateau, increased the catalytic activity in the diversity of the immune response [7]. Based on the results, we immunized mice for a long period with a TSA hapten, *N*-MMP **1** (Fig. 1), that was designed to mimic the distortion of porphyrin toward a transition-state geometry for insertion of a metal ion into porphyrin [8]. Fourteen hybridoma cell lines producing anti-**1** IgG were established [9],[1] although the hapten is known to generate a huge IgM response [10]. The catalytic activities of all the antibodies were examined for insertion of a cupric ion into mesoporphyrin (MP) **2** to produce cupric-mesoporphyrin (MP-Cu) **3** (Fig. 1). Two of them (antibodies **2B4** and **2D7**) accelerated the metalation reaction efficiently [9]. Further study

[1] In the reference, we reported that fifteen hybridoma cell lines secreting anti-**1** antibodies were obtained, but one of them could not be sustained.

revealed that three of them (**1F2**, **1F9** and **2H4**) also promoted the reaction at a rate above that of the background (unpublished results).

In the present work, to obtain information about what factor is responsible for the catalytic activity, we characterized and compared the properties of the five catalytic antibodies and the nine non-catalytic ones in the following aspects: (1) affinity to hapten **1**, (2) affinity to *N*-MMP-Fe **4** (Fig. 1) as a positively charged and metallic TSA, (3) orientation of the distorted porphyrin in the antigen-binding site, (4) peroxidase-like activity of the antibodiy·**4** complexes and (5) the primary structures of the complementarity-determining regions (CDRs) of the antibodies.

Based on the results obtained, we propose that Asp(H96) in CDRH3 is the key residue responsible for both the metalation and peroxidase-like activities of the antibodies.

2. Experimental

2.1. Materials

Porphyrin derivatives **1**, **2** and **4** were synthesized as described previously [9]. Monoclonal antibodies elicited against **1** were prepared and purified from ascites fluid as in the previous report [9]. The protein concentration was determined from the absorbance at 280 nm and calculated assuming A_{280} of 1% of IgG as 13.7 [11]. The antibody concentration was expressed per binding-site assuming a molecular weight of 150,000 (two binding sites per antibody). The buffer used consisted of 0.5% (w/v) Triton X-100, 5% (v/v) dimethyl sulfoxide and 90 mM Tris–acetate (pH 8.0). All other reagents were of analytical grade.

2.2. Determination of dissociation constants

Dissociation constants of **1** and **4** from the antibody, K_{d1} and K_{d4}, respectively, were estimated using a competitive enzyme-linked immunosorbent assay (ELISA), as previously reported [9]. The dissociation constants of cyanide from the antibody·**4** complex, K_{d4CN}, were determined based on the absorption change according to the previously described method [12].

2.3. Measurement of metalation activity

Catalytic activity for insertion of a cupric ion into **2** was determined by measuring the increase in absorbance due to the production of **3** [9]. The reaction mixtures contained 0.5–2 μM antibody, 10–50 μM of **2** and 0.5–2 mM Cu^{2+} acetate (Nacalai Tesque) in the buffer consisting of 0.5% (w/v) Triton X-100, 5% (v/v) dimethyl sulfoxide and 90 mM Tris–acetate (pH 8.0). Each reaction was initiated by the addition of Cu^{2+} solution. The time course of the absorbance change was followed at 397 nm in a cuvette of 0.1 cm path length at 37 °C. From the time course, the initial rate was calculated on the basis of the difference absorption coefficient at 397 nm between **2** and **3**, 0.318 $\mu M^{-1}\,cm^{-1}$ [9] and expressed as μM of **3** produced per minute. The initial rates obtained were corrected for the background rate. We previously predicted that the metalation reaction proceeds by the following scheme [9].

$$\text{Antibody} + MP \underset{K_s}{\rightleftarrows} \text{antibody} \cdot MP$$

$$\text{Antibody} \cdot MP + Cu^{2+} \underset{k}{\rightleftarrows} \text{antibody} + MP\text{-}Cu$$

where K_s is the dissociation constant of the antibody·MP complex and k the second-order rate constant for Cu^{2+} binding. From the scheme, the initial rate (v) is described as

$$v = \frac{k[\text{antibody}]_0[MP][Cu^{2+}]}{K_s + [MP]}. \quad (1)$$

If $K_s \gg [MP]$, v is given by the following equation.

$$v = \frac{k[\text{antibody}]_0[MP][Cu^{2+}]}{K_s} \quad (2)$$

2.4. Measurement of peroxidase-like activity

Peroxidase-like activity was measured by use of hydrogen peroxide and *o*-dianisidine as substrates according to the previously reported method [13]. Hydrogen peroxide solution (6 mM) was added to a cuvette of 0.1 cm light path length containing 0.76 mM *o*-dianisidine and 0.3 μM of the antibody·**4** complex. The concentration of the complex was expressed as that of the added **4** in a large excess of the antibodies, in which 95% of the added **4** was calculated to be bound to the antibodies by use of the K_{d4} values obtained. Initial rates were detected by following an

increase in absorbance at 500 nm and 10 °C, and expressed as M min^{-1} by using the absorption coefficient of the oxidized *o*-dianisidine, 6360 M^{-1} cm^{-1} [13].

2.5. Nucleotide sequence analyses

Nucleotide sequencing was carried out following the previously described strategy for sequencing of antibody **2B4** [13]. The mRNAs from **2D7**, **2H4**, **1F2** and **1F9** hybridoma cells were isolated from 10^7 cells by using a QuickPrep Micro mRNA Purification Kit (Pharmacia Biotech). Variable domains of the light and heavy chains (V_H and V_L) specific cDNAs were synthesized using a First-Strand cDNA Synthesis Kit (Pharmacia Biotech) with primer H3 (5′-GG***AAGCTT***A(T/C) CTCCACACAC AGG(A/G)(A/G)CCAGT GGATAGAC-3′ with the additional *Hind*III site in bold italics) or primer L3 (5′-GG***AAGCTT***AC TGGATGGTGG GAAGATGGA-3′ with the additional *Hind*III site in bold italics) [14]. Sense primer H5 (5′-GG***GAATTC*** TCTCTTCCTCCT GTCAG(T/G)AACT GCAGG-3′ with the additional *Eco*RI *site*) for **1F2** and **1F9** or H5′ (5′-GG***GAATTC***GA TGTCCAGCT(T/G) CA(A/G)CA(A/G)TC(A/T)G GACCT-3′ with the additional the *Eco*RI *site*) for **2D7** and **2H4** and reverse primer H3 were used to amplify selectively the V_H region by PCR (Taq DNA polymerase on a PJ2000 Thermal Cycler, Perkin-Elmer). To amplify the V_L region, PCR was run using L5 (5′-GG***GAATTC***TC TTCTGCTCTG GGT(A/G)TCTGGT GC-3′ with an additional *Eco*RI site) for **1F2**, **1F9** and **2D7** and L5′ (5′-GG***GAATTC***GA GTCACAG(A/T)(T/C)T CAGG(T/C)(A/C)TTTG TA-3′ with an additional *Eco*RI site) for **2H4** and L3 reverse primers. The amplified DNA was digested with *Hind*III and *Eco*RI and subcloned into the pUC18 vector. The pUC clones were sequenced by the dideoxy chain termination method using a Dye Primer Cycle Sequencing Ready Reaction Kit with AmpliTaq DNA polymerase CS+ (Perkin-Elmer) and an ABI 373S DNA sequencer (Perkin-Elmer). For each sequence of V_H and V_L, five clones were sequenced and aligned to construct consensus sequences.

Nucleotide sequences of non-catalytic antibodies were analyzed as follows. Total cellular RNA was extracted from the hybridoma cells producing the respective antibodies using TRIzol (Gibco BRL), and cDNAs were generated with oligo-dT primer using a cDNA cycle kit (Invitrogen). The 5′ primers for PCR were designed from N-terminal amino acid sequences determined in this study as follows: V_L for **2H10** (GACATTGTGC T(C/T/G)ACCCAGTC T), V_L for **1B7** and **1B8** (GACGT(C/G)(T/C)T(G/T/C)A TGACCCAGAC), V_L for **1B6**, **1C8**, **1F8**, **2H9** and **2H7** (GACATTGTGA TGACCCAGTC T), V_L for **2C2** (GA(A/G)AA(T/C)GTGC T(C/G/T)ACCCAGTC T), V_H for **2H10** and **2C2** (GAGGTCAA(A/G)C TGGT(C/G)GA(G/A)TC T), V_H for **1B6**, **1B7**, **1C8** and **2H7** (GAGGTCCAGC TGCA(A/G)GA(A/G)TC T) and V_H for **1F8** and **2H9** (GA(C/T)GTCCAGC TGGT(C/G)CA(G/A)TC T). The sequences of PCR 3′ primers were designed from the published sequences [14], as V_L (ACTGGATGGT GGGAAGATGG A) and V_H (A(T/C)CTCCACAC ACAGG(A/G)(A/G)CCA G), respectively. Nucleotide sequencing of the amplified DNA was carried out by the dideoxy chain termination method at Hokkaido System Science Co. Ltd. (Sapporo, Japan) and in our laboratory.

3. Results and discussion

In the previous study [9], we obtained five catalytic and nine non-catalytic antibodies that arose from the same immune response to a TSA hapten **1** for porphyrin metalation reaction. In order to determine the features responsible for the catalytic activity, we characterized the properties of the catalytic and non-catalytic antibodies.

3.1. Affinity to N-MMP

The rate acceleration by antibody **2B4**, which has the highest activity of the five catalytic antibodies, is ascribable to transition-state stabilization, and the structure of substrate porphyrin in the antigen-binding site of **2B4** is more distorted than that of free porphyrin [9]. To ascertain whether the rate acceleration by the other catalytic antibodies, **1F2**, **1F9**, **2D7** and **2H4**, is due to the transition-state stabilization, we studied the relationship between the kinetic parameter for the metalation reaction, k/K_s, and the dissociation constant of TSA hapten **1**, K_{d1}.

The initial rates for insertion of Cu^{2+} into MP **2** to produce MP-Cu **3** increased linearly with an increase

Table 1
Parameters of monoclonal antibodies elicited against *N*-methyl mesoporphyrin

Antibody	Dissociation constant			Metalation activity	Peroxidase activity
	N-MMP	*N*-MMP-Fe	Cyanide[a]	k/K_s ($\mu M^{-1}\,h^{-1}$)	v (μM/min)[b]
	K_{d1} (μM)	K_{d4} (μM)	K_{d4CN} (mM)		
1F2	0.015	0.11	2.0	0.0067	18
1F9	2.3	34	1.8	0.0025	22
2B4	0.0082[c]	0.031[d]	1.5[d]	0.33[c]	36
2D7	0.019	0.17	4.4	0.094	14
2H4	0.14	0.0018	0.64	0.021	13
1B6	0.3	0.45	0.92	UD	5.8
1B7	0.00056	0.047	1.8	UD	4.4
1B8	0.0044	0.0073	2.6	UD	4.2
1C8	0.0016	0.0089	0.13	UD	7.7
1F8	0.0018	0.017	2.0	UD	8.9
2C2	0.029	2.5	1.6	UD	5.9
2H7	0.22	9.1	2.3	UD	6.6
2H9	0.043	2.0	0.018	UD	8.6
2H10	0.51	>100[e]	ND	UD	ND
N-MMP-Fe	ND	ND	1.6[d]	ND	8.5

ND: not determined; UD: under the limit of detection.
[a] The dissociation constant of cyanide from the antibody and *N*-MMP-Fe complex.
[b] The initial velocity of the antibody and *N*-MMP-Fe complex for oxidation of *o*-dianisidine utilizing hydrogen peroxide.
[c] The value is deduced from [9].
[d] The value is deduced from [12].
[e] The dissociation constant could not be estimated by competitive ELISA.

in the concentration of **2** at 1 mM Cu^{2+} (data not shown). Therefore, we obtained the individual values of k/K_s directly from the plots of the reaction rate against the concentration of **2** according to the Eq. (2) as described in the Section 2.3. The K_{d1} values were determined by competitive ELISA. The values obtained are given in Table 1. The plots of k/K_s versus k_{uncat}/K_{d1} (k_{uncat} is the rate of the uncatalyzed reaction [9]) are shown in Fig. 2, where a linear relationship with a slope of 0.83 was observed among the antibodies **1F9**, **2B4**, **2D7** and **2H4** ($\gamma = 0.99$). According to the transition-state theory, plots of k/K_s versus k_{uncat}/K_{d1} are linear and the slope of the line should be equal to 1.0 [15–17]. The value of 0.83 indicates that the rate acceleration of the antibodies is attributed to the transition-state stabilization provided by the antibody-TSA interactions. An exception is the antibody **1F2**, in which the catalytic activity was not so high as was anticipated from the K_{d1} value. An unknown factor might decrease the catalytic activity of **1F2**.

It is expected that the catalytic antibodies have higher affinity to **1** than the non-catalytic ones, since the rate acceleration is ascribable to the transition-state stabilization as described above. However, Table 1 clearly shows that the catalytic antibodies do not always have higher affinity to **1** than the non-catalytic ones. This result is different from the report by Takahashi et al. for esterolytic catalytic antibodies [6], in which the catalytic antibodies tend to have a lower dissociation constant for their TSA hapten than the non-catalytic ones. Our observation suggests that a factor other than the affinity to TSA is responsible to the difference between the catalytic and non-catalytic antibodies. To clarify this point, the following experiments were performed.

3.2. Affinity to N-MMP-Fe

In the metalation reaction, a positively charged metal ion is inserted into the distorted porphyrin to form the sitting-atop intermediate, i.e. charged and

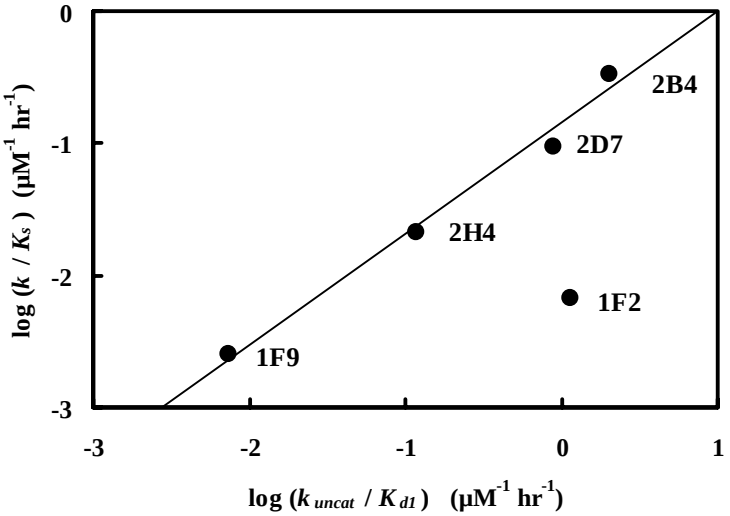

Fig. 2. Double logarithmic relationship between k_{uncat}/K_{d1} and k/K_s for the catalytic antibodies. The values of the K_{d1} and k/K_s are listed in Table 1 and $k_{uncat} = 0.0168\,h^{-1}$ at $[Cu^{2+}] = 1\,mM$ [9]. The line represents a linear relationship obtained among antibodies **1F9**, **2B4**, **2D7** and **2H4** with slope = 0.83 ($\gamma = 0.99$).

distorted metal-porphyrin [18]. When the antibody has no affinity to the distorted metal-porphyrin, it cannot accelerate the metalation reaction. To evaluate the affinity of the catalytic and non-catalytic antibodies, we measured the dissociation constant of ferric *N*-methyl mesoporphyrin (*N*-MMP-Fe **4**) from the antibodies, K_{d4}, by using competitive ELISA (Table 1) and showed the correlation between the K_{d4} and K_{d1} values in the plots of Fig. 3. It is found that all the antibodies except **2H10** have high affinity to **4** as well as **1**. This suggests that **2H10** has a positively charged residue in the binding site of the antibody whereas the other antibodies may have a negatively charged residue in the vicinity of the binding site.

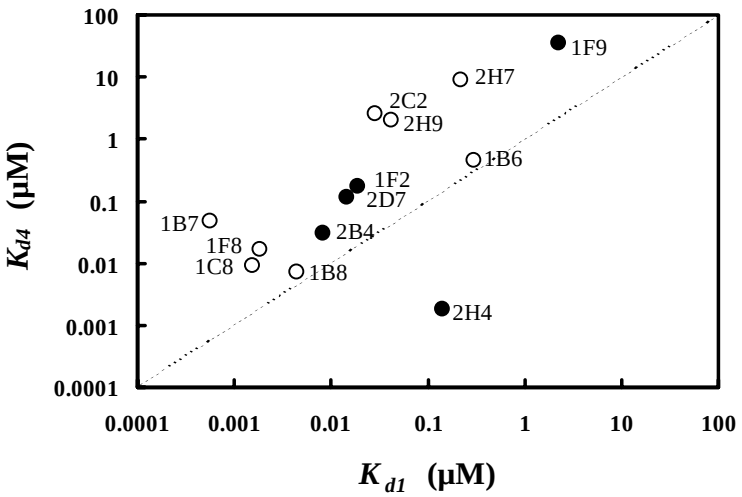

Fig. 3. Relationship between the dissociation constant of **1** (K_{d1}) and that of **4** (K_{d4}). The catalytic antibodies **1F2**, **1F9**, **2B4**, **2D7** and **2H4** (●) and the non-catalytic ones (○). The respective values are listed in Table 1. Dashed line represents the relationship of $K_{d1} = K_{d4}$.

3.3. Binding affinity of cyanide to ferric iron in the antibody·N-MMP-Fe complex

It is generally expected that the orientation of the distorted porphyrin in the antigen-binding site affects the catalytic activity. To clarify the relationship between the catalytic activity and the orientation of the porphyrin, the following experiments were performed.

The orientation of the distorted porphyrin in the antigen-binding site was evaluated by the binding affinity of cyanide to the antibody·**4** complex [12]; *N*-alkyl porphyrin with a metal ion exhibits a square–pyramidal coordination geometry, and an external ligand binds the metal ion at the apical position [19]. When cyanide binds the complex with a similar affinity to free **4**, we assume that the complex exposes the protruding side of **4** to solvents [12].

The dissociation constant of cyanide from the antibody·**4** complex, K_{d4CN}, was measured by the method described previously [12]. As shown in Table 1, the K_{d4CN} values of the complexes were similar to that of free **4**, indicating that the catalytic and non-catalytic antibodies expose the protruding site of the distorted porphyrin in the binding site to solvents.

3.4. Measurement of peroxidase-like activity

Catalytic antibody **2B4** shows another catalytic activity, a peroxidase-like one: it oxidizes *o*-dianisidine utilizing hydrogen peroxide when it combines with ferric porphyrin to form the antibody·ferric porphyrin complex [13]. A preliminary experiment showed that **2D7** also has the peroxidase-like activity. This observation gave us to the idea that the metalation activity associates with the peroxidase-like one. To confirm this, all the antibodies were examined in the peroxidase-like activity when they formed the respective antibody·**4** complexes.

As shown in Table 1 and Fig. 4, all the complexes of the catalytic antibodies accelerated their peroxidase-like activities at a rate above that of free **4**, while those of the non-catalytic antibodies had activities similar to **4**. This supports the above idea that the metalation activity closely relates to the peroxidase-like one. The results lead us to the view that the catalytic antibodies contain a common amino acid residue acting as catalyst for both the activities, and that an antibody lacking the residue should be non-catalytic for the reactions.

3.5. Primary amino acid sequences of antibodies

To see if there is any plausible amino acid residue in the antigen-binding sites of the catalytic antibodies, we determined the nucleotide sequences of their cDNAs and deduced the amino acid sequences. Fig. 5 shows the CDR sequences of the catalytic and non-catalytic antibodies. It is clear that all of the catalytic antibodies

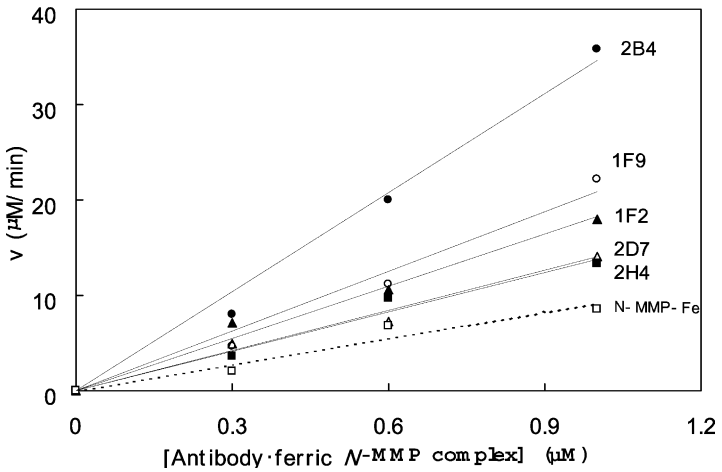

Fig. 4. Relationship between the initial rate of the peroxidase-like reaction and the antibody·ferric *N*-methyl mesoporphyrin complex. The concentration of the complex is expressed as that of the added ferric *N*-MMP in large excess of the antibodies. The reaction mixture contained 0.76 mM *o*-dianisidine and 6 mM hydrogen peroxide.

CDRL1

	Antibody	24	25	26	27	27a	27b	27c	27d	27e	27f	28	29	30	31	32	33	34
catalytic	**2B4**	K	A	S	Q	–	–	–	–	–	–	N	V	G	S	A	V	A
	2D7	·	·	·	·	–	–	–	–	–	–	I	·	·	·	N	·	·
	2H4	·	S	·	·	R	L	L	Y	R	S	·	Q	K	N	N	L	·
	1F2	·	·	·	·	–	–	–	–	–	–	·	·	·	T	V	·	·
	1F9	·	·	·	·	–	–	–	–	–	–	·	·	·	T	·	·	·
	7G12	·	·	·	·	–	–	–	–	–	–	·	·	·	T	P	·	·
		*		*	*													*
non-catalytic	**2H10**	R	·	·	K	S	V	S	T	–	–	S	G	Y	·	Y	M	H
	1B6	·	·	·	·	–	–	–	–	–	–	·	·	·	·	N	·	G
	1B7	R	S	·	·	T	I	K	A	T	–	Y	G	N	I	Y	L	E
	1C8	R	·	·	K	S	V	S	T	–	–	S	G	Y	·	Y	M	H
	1F8	·	·	·	·	–	–	–	–	–	–	D	·	·	A	·	·	G
	2C2	S	·	·	S	–	–	–	–	–	–	–	S	V	·	Y	M	H
	1B8	·	·	·	·	–	–	–	–	–	–	T	·	S	N	D	·	D
	2H9	·	·	·	·	–	–	–	–	–	–	D	·	·	T	·	·	G
	2H7	·	·	·	·	–	–	–	–	–	–	·	·	·	V	N	·	·

CDRL2

	Antibody	50	51	52	53	54	55	56
catalytic	**2B4**	S	A	S	I	R	Y	T
	2D7	·	T	·	S	·	·	S
	2H4	W	·	·	T	·	D	S
	1F2	·	·	·	·	·	·	N
	1F9	·	·	·	N	·	·	·
	7G12	·	·	·	N	·	·	·
				*		*		
non-catalytic	**2H10**	L	·	·	K	L	E	S
	1B6	·	·	·	Y	·	·	S
	1B7	K	V	·	N	·	F	S
	1C8	L	V	·	N	L	E	S
	1F8	W	·	·	T	·	H	·
	2C2	D	T	·	K	V	A	S
	1B8	Y	·	·	N	L	·	·
	2H9	W	·	·	T	·	H	·
	2H7	·	·	·	F	·	·	S

CDRL3

	Antibody	89	90	91	92	93	94	95	96	97
catalytic	**2B4**	Q	Q	Y	S	S	Y	P	L	T
	2D7	·	·	·	N	·	·	·	F	·
	2H4	·	·	·	Y	N	·	·	F	·
	1F2	·	·	·	·	·	·	·	F	·
	1F9	·	·	·	·	R	·	·	·	·
	7G12	·	·	·	·	·	·	·	·	·
		*	*	*			*	*		*
non-catalytic	**2H10**	·	H	S	R	E	V	·	·	·
	1B6	·	·	·	N	·	·	·	·	·
	1B7	F	·	G	·	H	V	·	F	·
	1C8	·	H	I	R	E	L	–	Y	·
	1F8	·	·	·	R	N	·	·	Y	·
	2C2	F	·	G	N	G	·	T	F	G
	1B8	H	·	D	Y	·	S	·	F	·
	2H9	·	·	·	R	K	·	·	Y	·
(A)	**2H7**	·	·	·	N	N	·	·	·	·

Fig. 5. Amino acid sequence alignment of CDRs in the monoclonal antibodies elicited against *N*-methyl mesoporphyrin as a hapten. (A) Light chain; (B) heavy chain. The sequences of antibodies **2B4** and **7G12** were deduced from [13] and [23], respectively. Points and dashes indicate identical amino acids and no amino acid, respectively. Asterisks (*) indicate homology found between the six catalytic antibodies. Underlines indicate tentative residues because a frame shift was observed in both the forward and reverse sequence analyses. The residue numbers above the sequences are indicated according to Kabat et al. [27]. The nucleotide sequence data reported were registered as DDBJ Accession nos.: AB090856 (H chain of **2H4**), AB090857 (H chain of **2D7**), AB090858 (H chain of **1F2**), AB090859 (H chain of **1F9**), AB090860 (L chain of **2D7**), AB090861 (L chain of **1F2**) and AB090862 (L chain of **1F9**).

CDRH1

	Antibody	31	32	33	34	35
catalytic	2B4	S	Y	G	M	H
	2D7	.	.	W	.	.
	2H4	.	.	W	.	.
	1F2	G	.	N	.	N
	1F9	E	.	T	.	.
	7G12	.	.	W	.	.
			*		*	
non-catalytic	2H10	.	.	D	.	S
	1B6	.	.	W	.	Q
	1B7	.	.	W	.	Q
	1C8	.	.	W	.	Q
	1F8	.	.	T	.	S
	2C2	.	.	T	.	S
	1B8	.	.	T	.	S
	2H9	.	.	T	.	S
	2H7	.	.	W	.	Q

CDRH2

	Antibody	50	51	52	52a	53	54	55	56	57	58	59	60	61	62	63	64	65
catalytic	2B4	Y	I	N	P	Y	N	A	G	T	K	Y	N	E	Q	F	K	G
	2D7	M	.	D	.	S	.	G	D	.	R	L	.	Q	K	.	N	D
	2H4	M	.	D	.	S	.	S	E	.	R	L	.	Q	K	.	.	D
	1F2	I	.	D	.	.	Y	G	.	.	T	.	.	Q	K	.	.	.
	1F9	G	.	.	.	N	.	G	.	.	S	.	.	Q	K	.	.	.
	7G12	M	.	D	.	N	S	G	.	.	.	.	.	.	K	.	.	S
			*		*					*			*			*		
non-catalytic	2H10	T	.	S	S	G	G	S	Y	.	Y	F	P	D	S	L	.	.
	1B6	E	.	.	.	S	.	G	R	I	N	.	.	.	K	.	.	N
	1B7	E	.	.	.	S	.	G	R	I	N	.	.	.	K	.	.	N
	1C8	E	.	.	.	S	.	G	R	I	N	.	.	.	K	.	.	N
	1F8	T	.	S	S	G	G	H	Y	.	Y	.	P	D	S	L	.	.
	2C2	T	.	S	S	G	G	H	Y	.	Y	.	P	D	S	L	.	.
	1B8	T	.	S	S	G	G	H	Y	.	Y	.	P	D	S	L	.	.
	2H9	T	.	S	S	G	G	H	Y	.	Y	.	P	D	S	L	.	.
	2H7	E	.	.	.	S	.	G	R	I	N	.	.	.	K	.	.	N

CDRH3

	Antibody	95	96	97	98	99	100	100a	100b	100c	100d	100e	100f	101	102
catalytic	2B4	R	D	G	-	-	-	-	-	-	-	-	-	D	Y
	2D7	.	.	M	-	-	-	-	-	-	-	-	-	.	.
	2H4	.	.	M	-	-	-	-	-	-	-	-	-	.	.
	1F2	.	.	M	-	-	-	-	-	-	-	-	-	.	.
	1F9	.	.	M	-	-	-	-	-	-	-	-	-	.	.
	7G12	.	.	M	-	-	-	-	-	-	-	-	-	.	.
		*	*											*	*
non-catalytic	2H10	H	R	D	H	Y	G	N	Y	Y	Y	V	M	.	.
	1B6	.	Y	S	-	-	-	-	-	-	-	-	-	.	.
	1B7	.	Y	S	-	-	-	-	-	-	-	-	-	.	.
	1C8	.	Y	S	-	-	-	-	-	-	-	-	-	.	.
	1F8	D	E	.	Y	Y	G	N	W	Y	F	-	-	G	V
	2C2	D	E	.	Y	Y	G	N	W	Y	F	-	-	G	V
	1B8	D	E	.	Y	Y	G	N	W	Y	F	-	-	G	V
	2H9	D	E	.	Y	Y	G	N	W	Y	F	-	-	G	V
(B)	2H7	.	Y	S	-	-	-	-	-	-	-	-	-	.	.

Fig. 5. (*Continued*).

use a homologous CDRH3 segment having the motif RDXDY. In contrast to the V_H segment homology, the V_L sequences of the antibodies are divergent.

This result suggests a fundamental significance of CDRH3 for the catalytic activities: namely, the presence of a key residue responsible for the activities in the region. It is generally recognized that CDRH3 has a crucial role in mediating the individual recognition of antigens, sometimes by changing its conformation upon antigen binding [20]. Shirai et al. [21] and Furukawa et al. [22] have proposed a novel classification of the CDRH3 conformation dependent on the sequence, though CDRH3 has variety in its length and amino acid sequence compared to the other CDRs. By applying their rule to our catalytic antibodies, the CDRH3 of the antibodies forms a type II β-turn with a kinked base and is stabilized by a salt bridge formed between Arg(H94) and Asp(H101), as shown in Fig. 6. In their conformation, the side chain of Arg(H95) will interact with adjacent Asp(H96) so as to position its carboxylic side chain. The structure agrees well with the X-ray crystallographic structure of the antibody **7G12** [23], which is elicited by hapten **1** and has both the metalation and peroxidase-like activities [8,24]. In the X-ray structure, the side chain of Asp(H96) is positioned by a hydrogen bond with Arg(H95), and the Asp(H96) lies in the vicinity of porphyrin ring at its center [23]. Since the CDRH3 sequence of **7G12** is identical to those of the catalytic antibodies presented here except **2B4** (Fig. 5), it is expected that the conformation of the CDRH3 in our antibodies resembles that of **7G12**. From this viewpoint, we anticipate that the residue of Asp(H96) may play a key role in the deprotonation of pyrrole nitrogen, facilitating the metal ion insertion into the porphyrin. The residue may also act as a general acid-base catalyst as the distal His of peroxidase does, as predicated by de Lauzon et al. in their peroxidase-like antibody **13G10** [25].

CDRH3

Antibody	93	94	95	96	97	101	102	103
2B4	A	R	R	D	G	D	Y	W
2D7	·	·	·	·	M	·	·	·
2H4	·	·	·	·	M	·	·	·
1F2	·	·	·	·	M	·	·	·
1F9	·	·	·	·	M	·	·	·

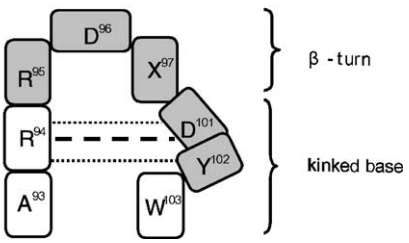

Fig. 6. A plausible schematic representation of the CDRH3 segments of the catalytic antibodies and amino acid sequence alignment around the CDRH3. The half filled ellipses are CDRH3 residues, and the broken and dotted lines indicates a salt bridge and hydrogen bonds, respectively.

From the above discussion, we propose that the factor that is essential to the catalytic antibodies for catalysis of the metalation and discriminates them from the non-catalytic antibodies is the presence of Asp(H96). Positioning the residue in the antigen-binding site may be critical to the activity. We surmise that the side-chain of Arg(H95) interacts with Asp(H96) to determine the orientation of a carboxylic side chain of Asp(H96) in the active site. This view is supported by the chemical modification experiments in which the antibodies **2B4** and **2D7** were reacted with carbodiimde and phenylglyoxal to decrease their catalytic activities [26]. To determine the role of Asp(H96) and Arg(H95), site-directed mutagenesis studies are now in progress.

4. Conclusions

Five catalytic antibodies for porphyrin metalation reaction were characterized and compared with nine non-catalytic antibodies in the following aspects; affinity to transition-state analogs, orientation of the analog in the antigen-binding site, peroxidase-like activity of the antibody-ferric porphyrin complex and the primary structure of the complementarity-determining regions of the antibodies. The results lead us to the view that the catalytic antibodies contain a common amino acid residue acting as catalyst for the activities, and that an antibody lacking the residue should be non-catalytic. We propose that the key residue is Asp(H96) in the third complementarity- determining region of the heavy chain.

References

[1] A. Tramontano, K.D. Janda, R.A. Lerner, Science 234 (1986) 1566.
[2] S.J. Pollack, J.W. Jacobs, P.G. Schultz, Science 234 (1986) 1570.
[3] H. Suzuki, J. Biochem. 115 (1994) 623.
[4] B. Golinelli-Pimpaneau, J. Immunol. Meth. 269 (2002) 157.
[5] D.S. Tawfik, B.S. Green, R. Chap, M. Sela, Z. Eshhar, Proc. Natl. Acad. Sci. U.S.A. 90 (1993) 373.
[6] N. Takahashi, H. Kakinuma, K. Hamada, K. Shimazaki, K. Takahashi, S. Niihata, Y. Aoki, H. Matsushita, Y. Nishi, Eur. J. Biochem. 261 (1999) 108.
[7] H. Suzuki, K. Sasaki, E.B. Mukouyama, Y. Kawamura-Konishi, Y. Wada, M. Ono, Biochem. Mol. Biol. Int. 34 (1994) 27.
[8] A.G. Cochoran, P.G. Schultz, Science 249 (1990) 781.
[9] Y. Kawamura-Konishi, N. Hosomi, S. Neya, S. Sugano, N. Funasaki, H. Suzuki, J. Biochem. 119 (1996) 857.
[10] G.R. Nakayama, P.G. Schultz, in: D.J. Chadwick, J. Marsh (Eds.), Proceedings of the Ciba Foundation Symposium on Catalytic Antibodies, vol. 159, Wiley, Chichester, New York, 1991, p. 72.
[11] D.A. Campbell, B. Gong, L.M. Kochersperger, S. Yonkovich, M.A. Gallop, P.G. Schultz, J. Am. Chem. Soc. 116 (1994) 2165.
[12] Y. Kawamura-Konishi, S. Neya, N. Funasaki, H. Suzuki, Biochem. Biophys. Res. Commun. 225 (1996) 537.
[13] Y. Kawamura-Konishi, A. Asano, M. Yamazaki, H. Tashiro, H. Suzuki, J. Mol. Catal., B Enzym. 4 (1998) 181.
[14] W.L. James, K.E. Fry, Methods 2 (1991) 106.
[15] T.S. Angeles, R.G. Smith, M.J. Darsley, R. Sugasawara, R.I. Sanchez, J. Kenten, P.G. Schultz, M.T. Martin, Biochemistry 32 (1993) 12128.
[16] J.D. Stewart, S.J. Benkovic, Nature 375 (1995) 388.
[17] H. Miyashita, T. Hara, R. Tanimura, S. Fukuyama, C. Cagnon, A. Kohara, I. Fujii, J. Mol. Biol. 267 (1997) 1247.
[18] M. Inamo, N. Kamiya, Y. Inada, M. Nomura, S. Funahashi, Inorg. Chem. 40 (2001) 5636.
[19] O.P. Anderson, A.B. Kopelove, D.K. Lavallee, Inorg. Chem. 19 (1980) 2101.
[20] A.R. Rees, S.J. Searle, A.H. Henry, N. Whitelegg, J. Pederson, in: M.J.E. Sternberg (Ed.), Protein Structure Prediction, Oxford University Press, New York, 1996, p. 141.
[21] H. Shirai, A. Kidera, H. Nakamura, FEBS Lett. 399 (1996) 1.
[22] K. Furukawa, H. Shirai, T. Azuma, H. Nakamura, J. Mol. Biol. 276 (2001) 27622.
[23] F.E. Romesberg, B.D. Santarsiero, B. Spiller, J. Yin, D. Barnes, P.G. Schultz, R.C. Stevens, Biochemistry 37 (1998) 14404.
[24] A.G. Cochoran, P.G. Schultz, J. Am. Chem. Soc. 112 (1990) 9414.
[25] S. de Lauzon, D. Mansuy, J.P. Mahy, Eur. J. Biochem. 269 (2002) 470.
[26] Y. Kawamura-Konishi, T. Aoki, N. Katagiri, H. Suzuki, in preparation.
[27] E.A. Kabat, T.T. Wu, H.M. Perry, K.S. Gottesmann, C. Foeller, Sequences of Proteins of Immunological Interest, fifth ed., US Department of Health and Human Services, National Institutes of Health, Bethesda, MD, 1991.